

Target Speed Estimation using Revised Range Point Migration for Ultra Wideband Radar Imaging

Takuya Sakamoto^{*†}, Toru Sato[†], Pascal Aubry^{*}, and Alexander Yarovoy^{*},

^{*}Delft University of Technology
Mekelweg 4, 2628CD Delft, the Netherlands
Email: T.Sakamoto@tudelft.nl

[†]Graduate School of Informatics, Kyoto University
Yoshida-Honmachi, Sakyo-ku, Kyoto, 606-8501 Japan

Abstract—Ultra wideband radar systems are of great interest in terms of applications to security surveillance systems in preventing crime where conventional camera-based systems cannot be used. Such systems require an antenna array with high-frequency switches to sequentially measure signals at different antenna positions. Targets are, however, not always cooperative in that during antenna scanning they might not be still. We propose a method for estimating target motion using the revised range point migration method and an image sharpness metric. The performance of the method is assessed by taking measurements of three moving targets: a corner reflector, a handgun and a knife in part to establish its applicability in detecting weapons.

Index Terms—radar imaging, target motion, sharpness metric

I. INTRODUCTION

Ultra wideband (UWB) radar imaging has been regarded as an indispensable technology for the next-generation security systems because of its high resolution and penetration through clothing, bags, and walls. Various imaging methods for UWB radar systems have been developed [1]–[7]. One important requirement for real-time security systems is computational speed, but many conventional imaging methods do not fulfill this requirement as usually the focus is only on imaging quality.

To improve computational speed during imaging, we developed the reversible inverse boundary scattering transform (IBST) [8]–[11] that directly calculates the target shape using quasi-wavefronts that are functions formed by the echo delay times. This avoids intensive computation as with many methods using optimization and migration processes. The IBST needs the derivative of the delay-time function in terms of antennae positions. This differential operation is, however, highly subject to noise and interference, which makes the IBST less competitive in practice.

To overcome this issue, the revised range point migration (RPM) method [12], [13] was developed which applies a weighted average using all neighboring peak points to calculate reliable derivative values. In computer simulations and measurements, the revised RPM method has been demonstrated to be fast and stable [12], [13].

However, conventional systems assume that targets remain still during scanning, which is not always the case in changing situations. Many such systems use array antennae and switches

to electronically scan the measurement position. Switching can take a long time, resulting in image blurring if the wrong motion of the targets is presumed. In this paper, we propose a method for estimating target motion using an image sharpness metric and the revised RPM algorithm. The performance of the proposed method is investigated by analyzing data from various moving targets, namely a corner reflector, a handgun, and a knife.

II. SYSTEM MODEL

We consider a three-dimensional (3-D) UWB radar imaging system. Figure 1 shows the system model assumed in this study. The measurement system consists of a transmitter-receiver pair positioned in the $z = 0$ plane along the x -axis at a fixed distance $2d$. The midpoint between the transmitter and receiver is labeled $(X, Y, 0)$. With the transmitter-receiver pair being rastered at discrete intervals across a portion of the $z = 0$ plane, UWB pulses are transmitted and pulse echoes are received. The received signals contain not only echoes from the target but also a coupling signal propagating directly from the transmitter to the receiver. To eliminate this coupling signal, the background signal, measured without the target prior to the actual measurement, is subtracted from the received signal. With antennae midpoint $(X, Y, 0)$, the signal received is denoted $s(X, Y, Z)$, where $Z = ct/2$. Here, c is the speed of the electromagnetic wave and t is the time interval between transmission and reception.

III. 3-D BISTATIC IBST

This section describes the procedures of the 3-D bistatic IBST [15], the basis of the revised RPM method. First, we extract signal peaks, which fulfill

$$\frac{\partial}{\partial Z} s(X, Y, Z) = 0, \quad (1)$$

$$|s(X, Y, Z)| > T_s, \quad (2)$$

where T_s is a constant threshold introduced to prevent noise being picked up. These peaks are indexed as (X_i, Y_i, Z_i) for $(i = 1, 2, \dots, N)$. The corresponding amplitudes of these peaks are for simplicity denoted $s_i = s(X_i, Y_i, Z_i)$. For a single simple-shaped target, these points are easily connected

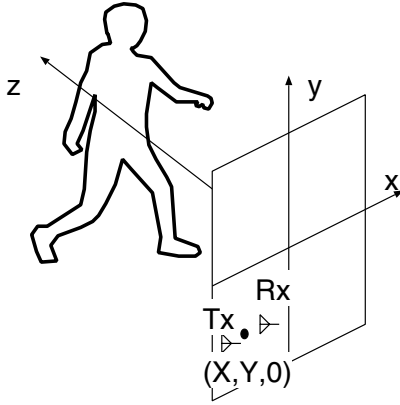


Fig. 1. System model with a pair of antennae scanning from the ($z = 0$) plane.

sequentially to form multiple curved surfaces $Z(X, Y)$. This function is called a quasi-wavefront.

Next, we apply the following bistatic-IBST to the quasi-wavefronts to obtain images.

$$x = X - \frac{2Z^3 Z_X}{Z^2 - d^2 + \sqrt{(Z^2 - d^2)^2 + 4d^2 Z^2 Z_X^2}}, \quad (3)$$

$$y = Y + Z_Y \{d^2(x - X)^2 - Z^4\} / Z^3, \quad (4)$$

$$z = \sqrt{Z^2 - d^2 - (y - Y)^2 - \frac{(Z^2 - d^2)(x - X)^2}{Z^2}}, \quad (5)$$

using for simplicity $Z_X = \partial Z / \partial X$ and $Z_Y = \partial Z / \partial Y$.

The bistatic-IBST requires accurate values of X, Y, Z, Z_X and Z_Y , of which X, Y and Z are known. To obtain derivatives Z_X and Z_Y , signal peaks need to be correctly connected. As this is not an easy task for complex-shaped targets, we defer using the bistatic-IBST.

IV. REVISED RPM METHOD

The RPM method [12] was developed to mitigate difficulties with the SEABED algorithm. To further enhance the processing speed, the revised RPM method [13] was proposed to sidestep the time-consuming optimization processes used in the conventional RPM method. This method employs a weighting average to quickly and accurately estimate the derivative of the delay time. The relative orientation of peaks around the i -th peak is estimated with a weighted average as

$$\theta_i = \frac{\sum_{j \neq i, Y_j = Y_i} w_{i,j} \tan^{-1} \left(\frac{Z_i - Z_j}{X_i - X_j} \right)}{\sum_{j \neq i, Y_j = Y_i} w_{i,j}}, \quad (6)$$

where the weighting function $w_{i,j}$ is defined as

$$w_{i,j} = |s_i s_j| \exp \left(-\frac{(X_i - X_j)^2}{\sigma_X^2} - \frac{(Z_i - Z_j)^2}{\sigma_Z^2} \right), \quad (7)$$

and $\left| \tan^{-1} \left(\frac{Z_i - Z_j}{X_i - X_j} \right) \right| < \pi/4$, and the summations are over pairs of peaks with the same sign in the second derivative, i.e.

$$s_{zz}(X_i, Y_i, Z_i) s_{zz}(X_j, Y_j, Z_j) > 0, \quad (8)$$

where $s_{zz}(X, Y, Z) = \frac{\partial^2}{\partial Z^2} s(X, Y, Z)$.

From this, we can estimate the partial derivative of the i -th range point in terms of X as $Z_X = \tan(\theta_i)$. In a similar way, we can estimate Z_Y . Finally, these derivatives are substituted into Eqs. (3), (4), and (5), to obtain target images.

The revised RPM method is known to be 170 times faster than conventional diffraction stack migration under a certain condition [13], and this speed is required for quick estimation because the imaging process is repeated many times.

V. SHARPNESS METRIC AND SPEED ESTIMATION

Images obtained with wrongly presumed motion are out of focus and blurred. This feature is used in our proposed method to estimate the motion of a target. The sharpness of an image can be evaluated with the Muller and Buffington (MB) sharpness metric [14]. The q -th order MB sharpness metric is calculated as

$$h_q = \frac{1}{M} \sum_{m=1}^M I_m^q, \quad (9)$$

where I_m is the m -th pixel or voxel of the image, and the order $q > 2$ is a constant that is set to $q = 4$ in this study.

If the image is well focused, the MB sharpness metric has a large value that can be exploited to estimate the target speed. We assume the target is moving at constant velocity, a valid assumption considering that moving targets do not change speeds within the short measurement periods. The method we propose produces multiple images corresponding to various assumed speeds, from which the maximum MB sharpness metric gives an estimate of the speed.

VI. APPLICATION TO MEASUREMENT

We applied our method to actual data obtained from three types of moving metallic targets: a dihedral reflector, a handgun and a knife. We used an Agilent PNA E8364B to sweep frequencies from 4.0 GHz to 20.0 GHz with 401 sampling points. The distance between the transmitting and receiving antennae was 5.5 cm, giving $d = 2.75$ cm. The antennae scanned at 1.0 cm intervals in an area of 50.0 cm \times 50.0 cm; the total number of measuring points was $51 \times 51 = 2601$. The antennae scanned from left to right while the target moved toward the antennae at a distance of either 38.0 cm or 19.0 cm. The target is placed on a moving platform that can be controlled electronically. These scenarios correspond to target speed of 1.0 m/s and 0.5 m/s, assuming a total measurement time of 0.38 s. Actually, our measurements took longer than the assumed measurement time because we recorded data in the frequency domain.

Zero-padding is applied in the frequency domain to generate oversampled data in the time domain with 900 samples. The maximum range covered with this measurement is 5.6 ns corresponding to 84 cm. The maximum number of quasi-wavefronts extracted is 15. The 3-D images generated with the RPM is $31 \times 51 \times 21$ in x, Y and z directions with a 0.5 cm grid size.

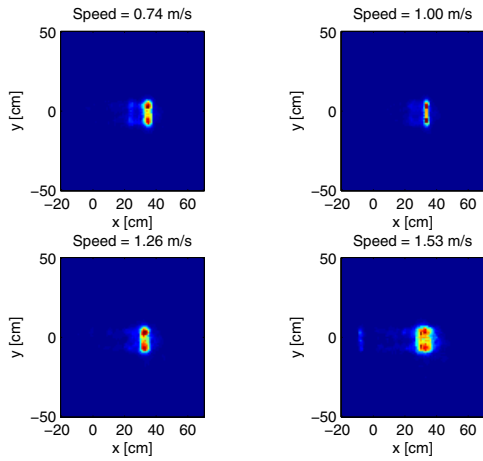


Fig. 2. Images obtained with the revised RPM method for various presumed speeds (actual speed is 1.0 m/s).

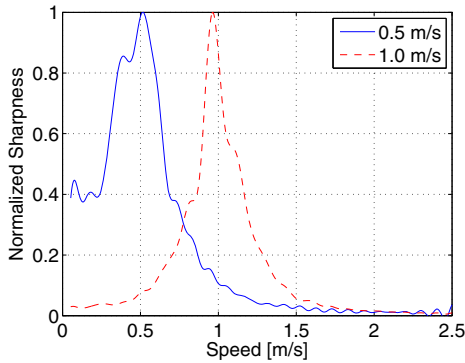


Fig. 3. Sharpness metric for a corner reflector moving at two different speeds (actual speeds are 0.5 m/s and 1.0 m/s).

Figure 2 shows radar images for the dihedral reflector generated using the revised RPM method for presuming different speeds; among these, the image corresponding to the actual speed of 1.0 m/s is the sharpest. We measured signals from the reflector twice at two different speeds. Figure 3 shows the fourth-order MB sharpness metric for various presumed speeds. The position of the peaks clearly show the correct speeds of the target. The estimated speeds are 0.52 m/s and 0.96 m/s respectively, corresponding to a 4% relative error. These results indicate that our method can estimate target speeds accurately for simple targets like a reflector.

Next, we apply our method to the targets with more complicated shapes: the handgun and knife. Figure 4 shows the photo of the handgun and knife used for our measurement. Figure 5 shows the sharpness metric for the handgun moving at 1.0 m/s. The peak of the sharpness metric is seen at 0.97 m/s, giving a 3% accuracy estimation. Figures 6 and 7 show the images generated using the diffraction stack migration with true and estimated speeds. Assuming the true speed is known, the first image generated shows a clear image of a handgun;



Fig. 4. Photo of a handgun and a knife used for our measurement.

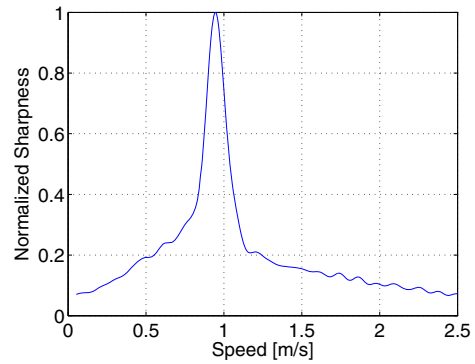


Fig. 5. Sharpness metric for a handgun moving at 1.0 m/s (maximum at 0.97 m/s).

assuming an estimated speed, the second figure also displays a clear 3-D outline that is easily recognizable as a handgun. This result indicates that the proposed method can estimate target speeds accurately enough for imaging, in particular, to applications related to weapon detection.

Figure 8 shows the sharpness metric for the metallic knife undergoing a similar motion at 1.0 m/s. The figure gives the estimated speed of 0.96 m/s, corresponding to a 4% accuracy.

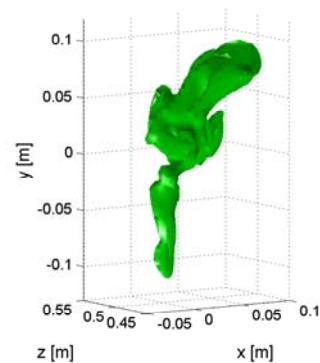


Fig. 6. Estimated target shape of a handgun using the actual speed (1.00 m/s). The scales are in meters.

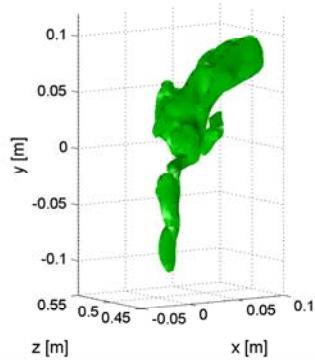


Fig. 7. Estimated target shape of a handgun using the estimated speed (0.97 m/s). The scales are in meters.

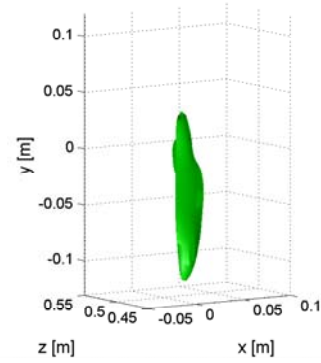


Fig. 10. Estimated target shape of a knife using the estimated speed (0.96 m/s). The scales are in meters.

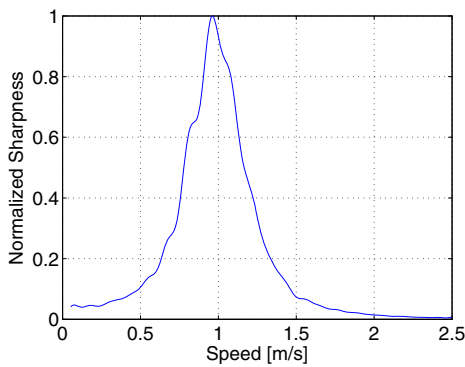


Fig. 8. Sharpness metric for a knife moving at 1.0 m/s (maximum at 0.96 m/s).

Figures 9 and 10 show images of the knife generated with the diffraction stack migration for the actual and estimated speeds, respectively. Both figures show a clear image of a knife, with differences being negligible.

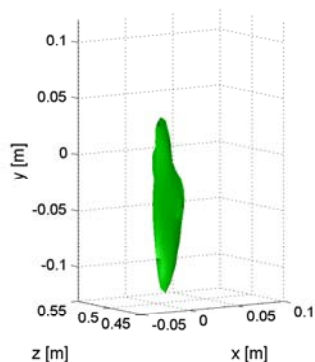


Fig. 9. Estimated target shape of a knife using the actual speed (1.00 m/s). The scales are in meters.

VII. DISCUSSION

The measurement setup affects the performance of the proposed method. For a larger antenna scan range, the estimation accuracy improves because radar data is more sensitive to the motion of targets. For targets farther from the antennae, estimation accuracies also improve because targets in the far-field are better approximated with a fewer number of point scatterers, making the focusing procedure easier.

VIII. CONCLUSIONS

We proposed an algorithm for estimating target speeds using the MB sharpness metric applied to images generated with the revised RPM method. This method presumes various speeds for the target to produce multiple images. For each image, the fourth-order MB sharpness metric is calculated to find the most focused image. We conducted measurements with a dihedral corner reflector, a metallic handgun and a metallic knife on a moving platform. The performance of the method was investigated with measurement data for speeds of 0.5 m/s and 1.0 m/s. As a result, for all of these three types of targets, our proposed method successfully estimated the speed of the target with a 3–4% accuracy. We also compared the images generated with the diffraction stack migration assuming actual and estimated speeds. For recognizing target shapes, the difference between the two images is negligible, indicating that the estimation accuracy of the speed is high enough from a practical sense. In actual security check applications, however, weapons are not open but can be hidden on the human body or concealed for example in a bag. These more complex scenarios require further investigation to assess the performance of our proposed method.

REFERENCES

- [1] A. G. Yarovoy, T. G. Savelyev, P. J. Aubry, P. E. Lys, L. P. Ligthart, "UWB array-based sensor for near-field imaging," *IEEE Transactions on Microwave Theory and Techniques*, vol. 55, no. 6, part 2, pp. 1288–1295, 2007.
- [2] X. Zhuge, A. G. Yarovoy, T. Savelyev, L. Ligthart, "Modified Kirchhoff migration for UWB MIMO array-based radar imaging" *IEEE Transactions on Geoscience and Remote Sensing*, vol. 48, no. 6, pp. 2692–2703, 2010.

- [3] X. Zhuge, and A. Yarovoy, "A sparse aperture MIMO-SAR based UWB imaging system for concealed weapon detection," *IEEE Transactions on Geoscience and Remote Sensing*, vol. 49 no. 1, pp. 509–518, 2011.
- [4] Y. Wang, Y. Yang, A. E. Fathy, "Experimental assessment of the cross coupling and polarization effects on ultra-wide band see-through-wall imaging reconstruction," *IEEE MTT-S International Microwave Symposium Digest*, pp. 9–12, 2009.
- [5] A. Nelander, "Switched array concepts for 3-D radar imaging," *Proc. 2010 IEEE Radar Conference*, pp. 1019–1024, 2010.
- [6] T. Counts, A. C. Gurbuz, W. R. Scott Jr., J. H. McClellan, and K. Kim, "Multistatic ground-penetrating radar experiments," *IEEE Trans. Geoscience and Remote Sensing*, vol. 45, no. 8, pp. 2544–2553, 2007.
- [7] Y. Yang and A. E. Fathy, "Development and implementation of a real-time see-through-wall radar system based on FPGA," *IEEE Trans. Geoscience and Remote Sensing*, vol. 47, no. 5, pp. 1270–1280, 2009.
- [8] T. Sakamoto, "A fast algorithm for 3-dimensional imaging with UWB pulse radar systems," *IEICE Trans. on Communications*, vol. E90-B, no. 3, pp. 636–644, 2007.
- [9] D. W. Winters, J. D. Shea, E. L. Madsen, G. R. Frank, B. D. Van Veen, S. C. Hagness, "Estimating the Breast Surface Using UWB Microwave Monostatic Backscatter Measurements," *IEEE Transactions on Biomedical Engineering*, vol. 55, no. 1, pp. 247–256, 2008.
- [10] S. Hantscher, A. Reizenzahn, C. G. Diskus, "Through-Wall Imaging With a 3-D UWB SAR Algorithm," *IEEE Signal Processing Letters*, vol. 15, pp. 269–272, 2008.
- [11] R. Salman, I. Willms, "In-Wall Object Recognition based on SAR-like Imaging by UWB-Radar," *Proc. 8th European Conference on Synthetic Aperture Radar (EUSAR)*, pp. 128–131, 2010.
- [12] S. Kidera, T. Sakamoto and T. Sato, "Accurate UWB Radar 3-D Imaging Algorithm for Complex Boundary without Range Points Connections," *IEEE Trans. Geoscience and Remote Sensing*, vol. 48, no. 4, pp. 1993–2004, 2010.
- [13] T. Sakamoto, T. G. Savelyev, P. J. Aubry and A. G. Yarovoy, "Revised Range Point Migration Method for Rapid 3-D Imaging with UWB Radar," *Proc. 2012 IEEE International Symposium on Antennas and Propagation and USNC-URSI National Radio Science Meeting*, 508.2, 2012.
- [14] R. A. Muller and A. Buffington, "Real-time correction of atmospherically degraded telescope images through image sharpening," *J. Optical Society of America*, vol. 64, no. 9, pp. 1200-1210, 1974.
- [15] S. Kidera, Y. Kani, T. Sakamoto and T. Sato, "A fast and high-resolution 3-D imaging algorithm with linear array antennas for UWB pulse radars," *IEICE Trans. on Communications*, vol. E91-B, no. 8, pp. 2683–2691, 2008.